Nicolas Riesen,Tess Reynolds, Alexandre François, Matthew R. Henderson, and Tanya M. Monro
Q-factor limits for far-field detection of whispering gallery modes in active microspheres
Optics Express, 2015; 23(22):28896-28904

Q-factor limits for far-field detection of whispering gallery modes in active microspheres

Nicolas Riesen,[1,*] Tess Reynolds,[1] Alexandre François,[1,2] Matthew R. Henderson,[1] and Tanya M. Monro[1,2]

[1]The Institute for Photonics and Advanced Sensing (IPAS) and ARC Centre for Nanoscale BioPhotonics (CNBP), School of Physical Sciences, The University of Adelaide, Adelaide, SA 5005, Australia
[2]University of South Australia, Adelaide, SA 5001, Australia
[*]nicolas.riesen@adelaide.edu.au

Abstract: This paper investigates the Q-factor limits imposed on the far-field detection of the whispering gallery modes of active microspherical resonators. It is shown that the Q-factor measured for a given active microsphere in the far-field using a microscope is significantly lower than that measured using evanescent field collection through a taper. The discrepancy is attributed to the inevitable small asphericity of microspheres that results in mode-splitting which becomes unresolvable in the far-field. Analytic expressions quantifying the Q-factor limits due to small levels of asphericity are subsequently derived.

OCIS codes: (140.3945) Microcavities; (230.5750) Resonators; (260.2510) Fluorescence.

References and links

1. M. L. Gorodetsky, A. A. Savchenkov, and V. S. Ilchenko, "Ultimate Q of optical microsphere resonators," Opt. Lett. **21**, 453-455 (1996).
2. T. J. Kippenberg, *Nonlinear optics in ultra-high-Q whispering-gallery optical microcavities* (CIT, 2004).
3. K. J. Vahala, "Optical microcavities," Nature **424**, 839-846 (2003).
4. A. François, N. Riesen, H. Ji, S. Afshar, and T. M. Monro, "Polymer based whispering gallery mode laser for biosensing applications," Appl. Phys. Lett. **106**, 031104 (2015).
5. F. Vollmer and S. Arnold, "Whispering-gallery-mode biosensing: label-free detection down to single molecules," Nat. Methods **5**, 591-596 (2008).
6. M. Himmelhaus and A. François, "In-vitro sensing of biomechanical forces in live cells by a whispering gallery mode biosensor," Biosens. Bioelectron. **25**, 418-427 (2009).
7. M. A. Gouveia, P. D. Avila, T. H. R. Marques, M. C. Torres, and C. M. B. Cordeiro, "Morphology dependent polymeric capillary optical resonator hydrostatic pressure sensor," Opt. Express **23**, 10643-10652 (2015).
8. B. E. Little, J.-P. Laine, and H. A. Haus, "Analytic theory of coupling from tapered fibers and half-blocks into microsphere resonators," J. Lightw. Technol. **17**, 704-715 (1999).
9. Y. Zhi, J. Valenta, and A. Meldrum, "Structure of whispering gallery mode spectrum of microspheres coated with fluorescent silicon quantum dots," J. Opt. Soc. Am. B **30**, 3079-3085 (2013).
10. H. T. Beier, G. L. Coté, and K. E. Meissner, "Modeling whispering gallery modes in quantum dot embedded polystyrene microspheres," J. Opt. Soc. Am. B **27**, 536-543 (2010).
11. Z. Ballard, M. Baaske, and F. Vollmer, "Stand-off biodetection with free-space coupled asymmetric microsphere cavities," Sensors **15**, 8968-8980 (2015).
12. H.-H. Yu, C.-H. Yi, and C.-M. Kim, "Mechanism for Q-spoiling in deformed optical microcavities," Opt. Express **23**, 11054-11062 (2015).
13. H. Lai, P. Leung, K. Young, P. Barber, and S. Hill, "Time-independent perturbation for leaking electromagnetic modes in open systems with application to resonances in microdroplets," Phys. Rev. A **41**, 5187-5198 (1990).
14. G. Kurizki, A. Kofman, A. Kozhekin, and G. Harel, "Control of atomic state decay in cavities and microspheres," New J. Phys. **2**, 28.1-28.21 (2000).
15. K. Srinivasan, O. Painter, A. Stintz, and S. Krishna, "Single quantum dot spectroscopy using a fiber taper waveguide near-field optic," Appl. Phys. Lett. **91**, 091102 (2007).
16. B. Redding, E. Marchena, T. Creazzo, S. Shi, and D. W. Prather, "Comparison of raised-microdisk whispering-gallery-mode characterization techniques," Opt. Lett. **35**, 998-1000 (2010).
17. N. Riesen, S. V. Afshar, A. François, and T. M. Monro, "Material candidates for optical frequency comb generation in microspheres," Opt. Express **23**, 14784-14795 (2015).

18. J. Zhang, L. Xue, and Y. Han, "Fabrication gradient surfaces by changing polystyrene microsphere topography," Langmuir **21**, 5-8 (2005).
19. H. Chew, "Radiation and lifetimes of atoms inside dielectric particles," Phys. Rev. A **38**, 3410-3416 (1988).
20. T. Reynolds, M. R. Henderson, A. François, N. Riesen, J. M. M. Hall, S. V. Afshar, S. J. Nicholls, and T. M. Monro, "Optimization of whispering gallery resonator design for biosensing applications," Opt. Express **23**, 17067-17076 (2015).
21. M. J. Humphrey, E. Dale, A. Rosenberger, and D. Bandy, "Calculation of optimal fiber radius and whispering-gallery mode spectra for a fiber-coupled microsphere," Opt. Comm. **271**, 124-131 (2007).

1. Introduction

Whispering gallery modes (WGMs), otherwise referred to as morphology dependent resonances, are optical modes propagating in resonators having at least one axis of revolution such as capillaries, disks or toroids, spheres and shells [1-4]. Light that is trapped by total internal reflection circulates inside the cavity close to the surface, and when returning in phase gives rise to resonance features. In recent years there has been growing interest in WGMs in part because the spectral positions of the resonances are strongly dependent on the refractive index contrast between the resonator and its surrounding environment, and this phenomenon has been exploited for refractive index sensing applications such as label-free biosensing [5]. Furthermore, the position of the resonances is also dependent on the geometry of the resonator, and this aspect has been used to measure e.g. resonator deformation induced by mechanical stress in various contexts [6, 7].

Several approaches have been used to excite and collect WGMs in microresonators such as microspheres, the most common being through a tapered optical fiber, phase-matched with the propagating WGMs in the resonator [2, 5, 8]. Recently, there has been emerging interest in the use of active microresonators, i.e. resonators that contain a gain medium, enabling either fluorescence [9, 10] or lasing of the WGMs [4]. Active microresonators permit the use of free-space excitation and collection of the WGMs, alleviating some of the practical issues related to the use of tapered fibers. The practical issues include fluctuation of the taper position with respect to the resonator which can result in increased spectral noise in the WGM signal, or the inevitable degradation of the transmission of the fiber taper from the fouling of the surface during e.g. biological sensing experiments [11]. Nevertheless, in most cases the WGMs excited and collected with a tapered fiber show extremely high Quality factors (Q-factors) ($\sim 10^5$ to 10^9) [1, 5], defined as the ratio between the wavelength position of the mode and its linewidth ($\lambda/\Delta\lambda$). In contrast, the vast majority of work in the literature involving far-field WGM collection from fluorescent microspheres reports Q-factors several orders of magnitude lower (500 to $\sim 10^4$) [4, 9, 10]. In this paper we demonstrate that a contributing factor to the difference is the increased role of geometric eccentricity on the spoiling of the Q-factor for far-field detection. This is in addition to the role of spectral broadening and fluorescence emitter linewidth in decreasing the Q-factor for active resonators [9].

In a recent paper by Yu *et al.* [12], a numerical demonstration was given of the spoiling of the Q-factor in disks resulting from small deformations. In this paper, we consider the case of spherical resonators, and it is shown that for active microspheres the spoiling of the Q-factor due to geometric eccentricity involves a different mechanism. We demonstrate that the collection scheme of the WGMs (tapered fibers vs far-field) from a given active microsphere plays a significant role in determining the measured Q-factor. This is a consequence of WGMs having spectral positions that are highly dependent on the resonator's morphology as stated above, and the fact that a microsphere is never perfect, always having a certain degree of asphericity. The asphericity essentially lifts the degeneracy between modes of different polar number resulting in 'mode-splitting,' in which the modes have unique resonance frequencies [6, 13, 14]. The split in modes is unique to different planes, all of which are excited in the case of an active microsphere. The difference between taper and far-field collection is that the highly mode-selective nature of the taper allows for the collection of a much smaller subset of polar modes, that are confined to a single equatorial plane [8]. In the case of far-field collection a near-continuum of split-modes from multiple planes are sampled

indiscriminately. This results in linewidth broadening and hence a reduction in the effective Q-factor.

2. Experimental results

These hypotheses are investigated in this paper by comparing taper and far-field sampling of the WGMs of active microspheres excited in both cases by free-space illumination. The reduction in Q-factor of active microspheres in the far-field due to asphericity is also modelled numerically, and a novel Q-factor component is derived to take into account the spoiling of the cavity Q-factor.

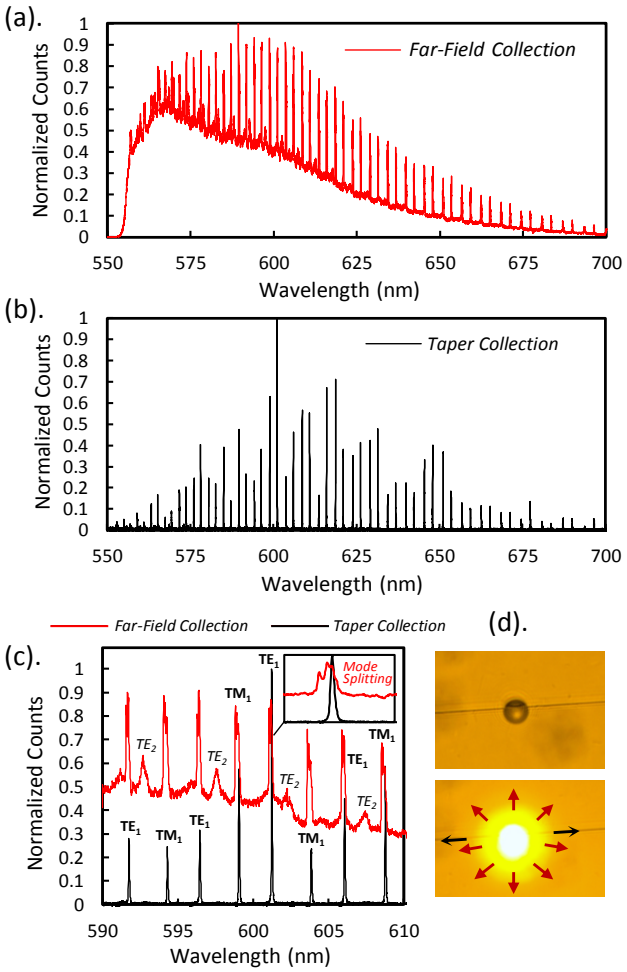

Fig. 1. (a)-(b) Whispering gallery mode spectra sampled in the far-field (red) and via the taper (black) of the same dye-doped polystyrene microsphere excited with free-space illumination. The measurements were taken simultaneously at the same pump power. (c) A closer look at the whispering gallery mode spectra of the polystyrene microsphere, and signs of mode-splitting for far-field collection (inset). (d) Microscope images showing the taper and attached microsphere under free-space excitation.

In order to reach an unambiguous conclusion, we used an experimental setup [15, 16] where the WGM signal from a single active microsphere can be acquired simultaneously from both a phase-matched tapered optical fiber and in the far-field, ensuring identical settings for the comparison. To achieve that goal, a drop of dye-doped polystyrene microsphere solution

was placed onto a microscope glass slide positioned onto an inverted microscope (IX 71, Olympus, Japan) set up in a confocal arrangement, allowing for the simultaneous excitation and far-field collection of the fluorescent microspheres. A packaged 1 micron diameter fiber taper was fixed to a separate 3-axis stage, allowing for the fiber taper to be maneuvered independently above the glass slide and within the microsphere solution droplet. This allowed for the taper to be positioned in contact with single microspheres. The microspheres were prepared from non-fluorescent commercial polystyrene spheres in aqueous solution (Ø ~15 μm; n=1.59; Polysciences Inc., USA) by doping them with a fluorescent dye (Nile Red, λ_{abs} ~532 nm, λ_{em} ~590 nm, Sigma Aldrich) using a method described elsewhere [4]. The free-space excitation of the microspheres was achieved through the inverted microscope with a ×20 objective, using a λ ~532 nm CW laser as the pump source. The pump power at the focal point of the microscope objective was 3.0 mW with a spot size comparable with the microsphere's diameter (Ø~15 μm). For far-field collection, the emission was collected back through the same ×20 objective and coupled into a 200 μm patch fiber. For both WGM collection strategies (i.e. far-field vs tapered fiber), the WGM spectra were resolved with a spectrometer (iHR550, Horiba, Japan) equipped with a 2400 mm^{-1} grating and a cooled CCD (Synapse 2048 pixels, Horiba, Japan).

Figures 1(a) and 1(b) show the WGM spectrum of a single free-space illuminated microsphere collected in the far-field through the microscope and through the attached fiber taper, respectively. Microscope images of the microsphere and attached taper are given in Fig. 1(d). In both cases, the WGMs are clearly distinguishable, although the fluorescence background in the far-field spectrum of Fig. 1(a), is absent in the fiber taper collection spectrum of Fig. 1(b) as would be expected due to the negligible off-resonant coupling. The smaller, broad peaks visible in the far-field spectrum were identified as higher-order modes which do not couple efficiently with the taper. The highly mode-selective nature of tapers means that such discrepancies in far-field and tapered fiber transmission spectra are to be expected. A closer view of both spectra centered at 600 nm is provided in Fig. 1(c), highlighting the difference in linewidth and therefore Q-factor measured for the same microsphere excited at the same pump power, but collected in two different ways. This result demonstrates the significant dependence of the measured Q-factor on the collection mechanism used. In the case of far-field collection the Q-factor is ~2600, whereas for taper-collection for the same microsphere at the same time and under the same excitation conditions yields a Q-factor of ~12,600. This approximately five-fold increase in Q-factor was consistent amongst many microspheres tested. Note that the presence of the taper appeared to have negligible influence on the far-field Q-factor, with no change observed upon attachment. Furthermore the measured Q-factors were steady suggesting minimal spectral noise due to motion of the sphere or taper.

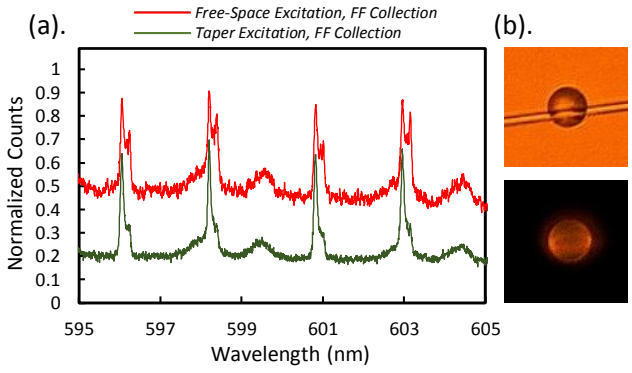

Fig. 2. (a) Whispering gallery mode spectra sampled in the far-field of the same dye-doped polystyrene microsphere excited with either the taper (green) or with free-space illumination (red). (b) Microscope images showing taper excitation of the microsphere with the pump wavelength removed using a dichroic filter.

Given the clear difference in Q-factor for the two different collection schemes (i.e. taper vs far-field) we also investigated the influence of the excitation mechanism. This involved comparing the far-field collected spectrum of an active microsphere for free-space (red curve) and taper excitation (green curve) as shown in Fig. 2. In this case the Q-factor is improved by only a factor two when using the taper.

As seen in Fig. 2(b) the WGMs of the active microsphere excited with the taper are more spatially confined than is observed for free-space excitation (see Fig. 1(d)). However since the fluorescent dye emits in all directions the WGM confinement to a single plane is weak. The Q-factor improvement using taper excitation is less significant than when using taper collection (i.e. Fig. 1), due to both the near indiscriminate emission of the dye into various WGMs/planes of the sphere regardless of the excitation technique and the indiscriminate sampling occurring for far-field collection. This results in a larger number of near-degenerate modes being sampled than for taper collection, which overlap to contribute to linewidth broadening. Compared with free-space excitation, the mode-splitting is more clearly evident here due to the smaller subset of modes/planes excited when using taper excitation. The dual-peak resonances in Fig. 2 are indicative of an ellipticity in the resonator [13]. Note also that the higher-order modes are present in both spectra due to the indiscriminate nature of far-field sampling.

3. Theoretical analysis

In the following section we propose and model a Q-factor component for an active microsphere due to a given degree of asphericity, assumed to be small, for free-space WGM excitation and collection. This Q-factor component (denoted here by Q_{FF}) contributes to the overall cavity Quality factor through the usual expression, $Q^{-1} = \sum 1/Q_i$, where Q_i are the individual components accounting for radiative losses from the curved microsphere surface (Q_{geo})[17], scattering losses due to surface in-homogeneities (Q_s), material losses (Q_{mat})[1, 17], and as mentioned, the asphericity of the microsphere (Q_{FF}).

In the case of the polystyrene microspheres, $Q_s \sim 10^6$ assuming a surface roughness with correlation length and variance of 25 nm [18]. In the extreme case of a correlation length and variance of 50 nm, the Q-factor due to scattering reduces to $Q_s \sim 6\times10^4$, which is still significantly higher than the measured Q-factor. The Q-factor due to material losses [1] is $Q_{mat} \sim 10^7$, assuming an attenuation coefficient of $\alpha_m = 0.3$ dB/m. The Q-factor due to tunneling or radiation losses determined using the Chew model is $Q_{geo} \sim 2\times10^5$ [19]. In our experiments the resolution of the spectrometer was 4 pm, equivalent to a maximum Q-factor that can be resolved at 600 nm of $Q_{spect} \sim 5\times10^4$. The measured Q-factor ($Q \sim 10^3$) for far-field collection is however consistently far lower than any of these Q-factor components even with conservative estimates. As mentioned, the discrepancy can in part be attributed to the slight asphericity of the resonator.

Two different approaches were adopted for modeling the Q-factor spoiling due to the asphericity (Q_{FF}). The first involved modelling the excitation of many sphere planes with slightly varying radii, and the second involved modelling polar mode-splitting of a single plane due to an elliptical distortion of the sphere (as described in [13]).

3.1 Multiple-Plane Model

The spoiling of Q-factor by the free-space excitation and collection of resonances from multiple sphere planes of slightly different radii was modeled by calculating the wavelength shift of the most sensitive resonances of a perfect sphere, i.e. the first-order fundamental ($m = l$) modes, as the radius ρ, is varied over a range $\Delta\rho$. Since multiple planes are excited indiscriminately in an active microsphere, the result is the sampling of almost a continuum of slightly perturbed resonances, which superimpose to broaden the initial resonances, hence resulting in the dramatic reduction in the Q-factor. The corresponding Q-factor component (Q_{FF}) can be approximated by $\lambda/\Delta\lambda$, where λ is the wavelength of a given fundamental mode,

and $\Delta\lambda$ is the range of resonance wavelength perturbations across all sampled WGM planes. For very small perturbations, the value $\Delta\lambda$ can be determined simply from the range of effective radii over all sampled planes, $\Delta\rho$. Here effective radius is simply the radius of a perfect sphere with circumference equal to the boundary of a given irregular plane. If there is a continuum of radii within the range $\Delta\rho$ for all the excited/sampled planes, the modes overlap and broaden the initial linewidth resulting in a reduction of the effective Q-factor.

Assuming that $l \sim 2\pi\rho n/\lambda$ which is an appropriate estimate for e.g. the fundamental modes in the limit of $l >> 1$, an approximation of Q_{FF} for an active microsphere is,

$$Q_{FF} = \frac{\omega}{\Delta\omega} \approx \frac{\rho}{\Delta\rho} \tag{1}$$

This expression is given by the black line in Fig. 3(b) for ρ = 7.5 μm. This far-field Q-factor component (Q_{FF}) is not dependent to first-order on the specific wavelength or refractive index contrast, whereas it is proportional to the size of the microsphere. For a given level of asphericity $\Delta\rho$, the value of Q_{FF} decreases with smaller sphere size, as might be expected. Note however that the influence of Q_{FF} on the overall Q-factor is likely to be less significant for very small microspheres ($\rho \sim\lambda$) or small refractive index contrast Δn, due to the inherently low Q_{geo} to begin with.

At this point it should be noted that since far-field detection relies on radiative tunneling losses (or surface scattering) the collection mechanism tends to become inefficient for large ρ, such that the resonances might no longer be detected [16]. This is one of the reasons why tapered fiber collection is prefered for large microspheres. Far-field collection can only be used in the regime where radiative bending losses are greater or comparable to the internal loss mechanisms of the resonator or when scattering losses are high [16], and the models presented in this paper are limited in practice to this regime.

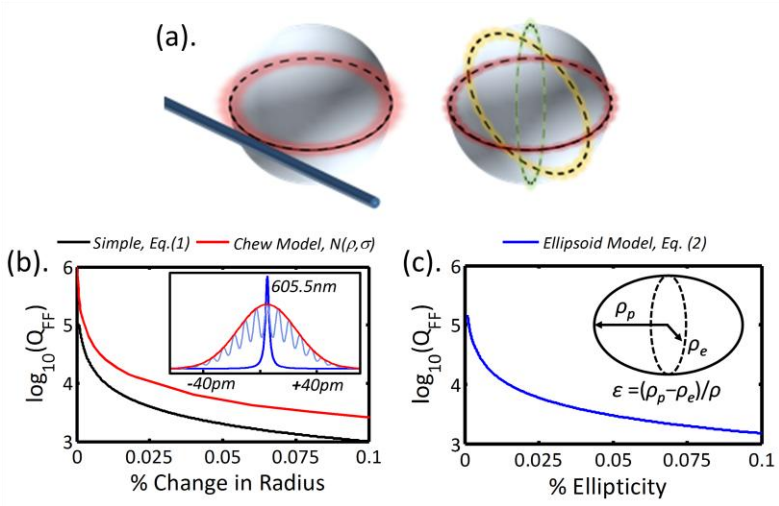

Fig. 3. (a) Depiction of the fiber taper and far-field collection of the WGM signal of the microsphere. Quantification of the spoiling of the Q-factor of an active microsphere when using far-field excitation and collection by (b) modelling the wavelength shift over a range of radii $\Delta\rho$ of a perfect microsphere or (c) the wavelength shift associated with mode-splitting for given levels of ellipticity ε. The inset of (b) shows the Q-factor spoiling occurring for a Gaussian distribution of radii with mean 7.5 μm and standard deviation σ = 0.5 nm modelled using the Chew model [19, 20]. Here the dark blue curve is the fundamental mode for a perfect sphere, whereas the light blue peaks are the non-degenerate fundamental ($m = l$) modes for an aspherical resonator, which overlap to yield linewidth broadening as suggested by the red Gaussian fit.

The Q-factor spoiling was also calculated numerically using the same approach as before, but this time using the Chew model [19, 20]. WGM spectra of perfect spheres were generated for a range of radii $\Delta\rho$ and then summed, with the spectrum generated for each radius weighted with respect to the radii distribution used. Here a normal distribution was used (compared with a uniform distribution assumed for Eq. (1)) such that the range $\Delta\rho$ corresponds to radii within 3 standard deviations of the mean, i.e. with mean ρ and standard deviation $\sigma = \Delta\rho/6$. The Q_{FF} component based on $\lambda/\Delta\lambda$ was calculated from the summed spectrum by fitting a Gaussian distribution. An example calculation is shown in the inset of Fig. 3(b) for $\sigma = 0.5$ nm. The resulting Q-factors are shown by the red line in Fig. 3(b). The discrepancy with Eq. (1) arises due to the assumption of a normal distribution here which naturally yields higher Q-factor estimates for a given value of $\Delta\rho$.

We infer from Eq. (1) that if the variation in radius exceeds 190 picometres ($>2.5\times10^{-3}$%) for the polystyrene microspheres, the asphericity is likely to become the limiting factor on the Q-factor. For the experimental results the Q-factor measured (Q_{FF} ~2600) would suggest a 0.05% variation in radius equivalent to a plausible deviation of 3 nm across all equatorial planes.

3.2 Ellipsoid Model

The second approach for modelling the Q-factor degradation for far-field collection due to asphericity involves considering an ellipsoidal perturbation. Ellipticity of a microsphere lifts the degeneracy between the polar modes as described in [13], which can then effectively broaden the initial resonance peak. To determine the associated Q-factor component, we first consider the quantum numbers commonly assigned to the modes of a microsphere for a given equatorial plane. These are the radial q, angular l, polar m (where $|m| \leq l$), and polarization mode numbers p [8]. The radial and angular mode numbers determine the number of nodes in the radial and azimuthal directions, respectively, and the number of lobes in the polar direction is determined by $l-m+1$. The fundamental modes ($m = l$) usually dominate, and correspond to propagation closest to the equator of the sphere [8]. In a perfect microsphere the subspace of modes of given q, l and p but with different values of m is $2l+1$ fold degenerate. In practice the degeneracy is always lifted to some extent due to the asphericity of the microsphere resulting in a range of m-dependent frequencies. The asphericity essentially removes the degeneracy in path-length of modes with different polar order, m. Only a select number of these m-dependent modes of appropriate spatial confinement couple efficiently with an attached taper [8, 21]. In fact, using coupled mode theory it can be shown that the power coupled between a taper and the microsphere is proportional to $\exp(-\Delta\beta^2)$, where $\Delta\beta = \beta_f - m/\rho$ is the phase mismatch between taper and microsphere modes and β_f is the fiber modal propagation constant [8]. The exponential dependence implies that the taper-to-sphere coupling is highly mode-selective, as is well established, allowing for coupling with only a small subset of the m-dependent modes. The WGMs of lower polar order m also have wider polar distribution of the fields such that the spatial overlap with the taper modes is much lower. This can dominate over the phase mismatch since the propagation constants do not vary dramatically for different polar orders [8, 21]. The high mode-selectivity of the taper means that the mode-splitting is usually resolvable and evidenced by just a few different peaks in the sampled spectrum, with minimal linewidth broadening occurring [2, 13, 14]. For far-field collection there is no discrimination between different m-dependent modes (or different sphere planes). A large number of modes are therefore sampled, which partially overlap, resulting in linewidth broadening of the initial peak.

The expressions for mode-splitting in an ellipsoid of axially symmetric shape distortion are given by [13]. Assuming $l >> 1$, the relative shift in angular frequency due to an elliptical deformation (as defined in Eq. (1.2) of [13] with L = 2, M = 0) for polar mode m is [13],

$$\frac{\Delta\omega}{\omega} = \frac{\varepsilon}{6}\left(\frac{3m^2}{l^2} - 1\right) \qquad (2)$$

where $\varepsilon = (\rho_p - \rho_e)/\rho$ is the ellipticity, and ρ_p and ρ_e are the polar and equatorial radii, respectively. We assume here that the ellipticity is sufficiently small such that the modes partially overlap. If we take the final peak width to be the total range of individual polar mode shifts, by calculating the difference between the two extremes $m = 0$ and $m = l$, we find a width of $\Delta\omega = 2\varepsilon\omega/3$, yielding a Q_{FF} of $3/2\varepsilon$. Fig. 3(c) shows the slightly higher estimate in Q-factor predicted by this model. For the Q-factor of 2600 measured for the polystyrene microspheres, this model would suggest a microsphere ellipticity of $\varepsilon \sim 5.8\times10^{-4}$ (i.e. $|\rho_p - \rho_e| =$ 4 nm).

To determine whether the low levels of asphericity predicted by the two models are plausible, scanning electron microscopy (SEM) was used to image a number of the polystyrene microspheres. Samples were coated with a 5 nm platinum coating and imaged with a Quanta 450 SEM at a resolution of 4096 × 3775 pixels at ×5000 magnification. Images were then processed by adjusting the brightness/contrast, followed by the use of a threshold to obtain a two colour image of the sphere as shown in Fig. 4(b). An ellipse was then fit to each two colour sphere image using the Matlab image processing function "regionprops".

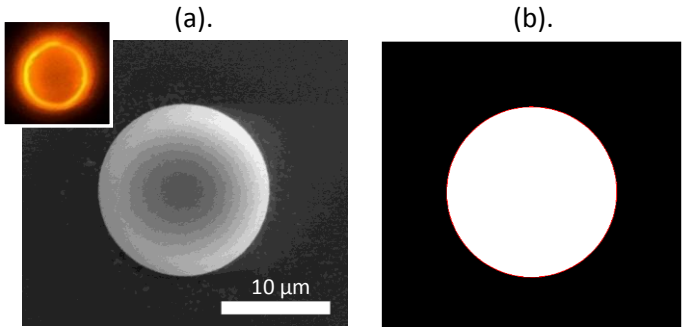

Fig. 4. (a) Low resolution scanning electron microscope (SEM) image of a 15 µm polystyrene microsphere. Inset shows the same sphere when excited by the taper (b) Corresponding two color threshold image with an ellipse fit shown (red line).

Over the seven samples measured, the difference in major and minor ellipse axes was 11 ± 4 pixels (corresponding to 80 ± 30 nm) with ellipse orientation of 2 ± 7°. Such a regular axis difference, with orientation consistently near 0°, is indicative of a systematic unequal aspect ratio of the imaging system (i.e. image stretching/contracting) rather than an actual ellipticity of the spheres. Compensating for this unequal aspect ratio, the ellipse fit was repeated for the spheres, yielding an average ellipticity of 4 pixels or 30 nm with random orientation. This level of ellipticity is at the detection limit of the measurement system and therefore represents an upper limit. It corresponds to a relative distortion of about 0.2% for the 15 µm spheres.

These SEM images demonstrate that the few nanometer asphericity suggested by the Q-factor spoiling in the far-field is plausible. The very low levels of asphericity are however very difficult to measure accurately, given the relatively large resonators considered. Indeed Q-factor degradation could be used as an indirect method of measuring such minute geometric asphericities. The SEM images also do not allow one to differentiate between the two models described. Note however that the two models merely represent two different ways of describing a small geometric perturbation, and yield nearly identical results.

4. Conclusions

This paper has investigated the Q-factor limits for active microspheres in the far-field due to slight asphericity. It has been shown that even minute geometric eccentricity of the order of tens of nanometers or less can significantly spoil the Q-factor for far-field collection. In this paper a Q-factor spoiling of more than a factor 5 is shown for 15 μm polystyrene microspheres due to a several nanometer eccentricity. Given these findings it is likely that the low Q-factors of active microspheres measured in far-field experiments could be mistaken for higher contributions from either scattering or material absorption. The technique of comparing both the far-field and evanescently coupled WGM signal from an active microsphere could be exploited for various applications including strain sensing in which very small cavity deformations could be measured [6].

Acknowledgments

The authors acknowledge the support of an Australian Research Council Georgina Sweet Laureate Fellowship awarded to T. M. Monro, FL130100044. We also acknowledge Adelaide Microscopy for the use of SEM facilities. M. R. Henderson was supported by a grant from the National Breast Cancer Foundation Australia, NC-13-05.